ACCURACY AND PERFORMANCE OF LINEAR UNMIXING TECHNIQUES FOR DETECTING MINERALS ON OMEGA/MARS EXPRESS

Frédéric Schmidt[1], Sébastien Bourguignon[2], Stéphane Le Mouëlic[3], Nicolas Dobigeon[4], Céline Theys[2] and Erwan Tréguier[5]*

[1]Univ Paris-Sud, Laboratoire IDES, UMR8148, Orsay, F-91405; CNRS, Orsay, F-91405 [2]Univ. Nice Sophia Antipolis, Laboratoire Fizeau, France [3]Laboratoire de Planétologie et Géodynamique, CNRS UMR6112, Université de Nantes, 2 rue de la Houssinière, 44300 Nantes, France, [4]University of Toulouse, IRIT/INP-ENSEEIHT, France [5]ESA, ESAC, Villanueva de la Cañada, Spain

ABSTRACT

Detecting minerals on a huge hyperspectral dataset (> To) is a difficult task that we proposed to address using linear unmixing techniques. We test different algorithms with positivity constrains on a typical Martian hyperspectral image of the Syrtis Major volcanic complex. The usefulness of additional constrains, such as sparsity and sum-to-one constrains are discussed. We compare the results with a supervised detection technique based on band ratio.

Index Terms— Hyperspectral imaging, supervised classification, linear unmixing, positivity, sum-to-one, sparsity, automatic detection, planetology, minerals, ice.

1. INTRODUCTION

In remote sensing hyperspectral imaging, a set of images is recorded at various spectral bands by the sensor which measures the solar light reflected and scattered back from the surface and from the atmosphere. Under some assumptions related to surface and atmosphere properties - i.e., Lambertian surface, no intimate mixture, no diffusion terms in the atmosphere, and homogeneous geometry in the scene - each measured spectrum (each pixel of the observed image for several spectral bands) can be modeled as a linear mixture of the scene component spectra (endmembers) [1]. In this model, the weight of each component spectrum is related to its abundance in the surface area corresponding to the underlying pixel.

By considering P pixels of an hyperspectral image acquired in L spectral bands, the observed spectra are gathered in a P × L data matrix **X**. The p^{th} row of this matrix contains the measured spectrum at a pixel with spatial index p (p = 1, . . . , P). According to the linear mixing model, the p^{th} spectrum can be expressed as a linear combination of R minerals spectra, i.e., surface reflectance spectra. Using matrix notations, this linear spectral mixing model can be written as:

$$\mathbf{X} \approx \mathbf{AS} \quad (1)$$

The R rows of the matrix **S** contain the surface pure spectra of the R components and each element $a_{p,r}$ of matrix **A** corresponds to the abundance of the r^{th} component in the pixel p.

The supervised linear unmixing problem consists of estimating matrix **A** knowing **X** and **S,** in contrary to unsupervised unmixing that consists of estimating matrix **A** and **S**, knowing only **X** [2]**.**

A first strong constraint is the non-negativity of the elements of **A** since they correspond to abundances of the surface components:

$$A_{p,r} \geq 0, \forall p,r \quad (2)$$

A second constraint that may be imposed is the sum-to-one (additivity) constraint on the abundances that should sum to unity for each pixels p:

$$\Sigma_r A_{p,r} = 1, \forall p \quad (3)$$

A third constraint that may be imposed is the sparsity of A, meaning that only a few spectra in the reference spectral library are present in each observed spectrum. That is, most abundances $A_{p,r}$ should be equal to zero. We consider the Basis Pursuit De Noising approach [3] to this problem, which consists in minimizing the least-squares criterion related to (1), penalized by the L1-norm of the coefficients:

$$\min \Sigma_r |a_{p,r}|, \forall p \quad (4)$$

Section 2. describes the reference spectra **S**. Section 3, describes the OMEGA observation used for the test. We test several algorithms summarized in section 4. Section 5 presents the results.

2. REFENCE SPECTRA

We used the following collection of laboratory reference spectra [4,5,6]:

* corresponding author: frederic.schmidt@u-psud.fr

List of minerals spectra:
(1) Hypersthene PYX02.h >250u, (2) Silicate (Ino) ; Diopside CPX CRISM, (3) Olivine Fayalite CRISM, (4) Olivine Forsterite CRISM, (5) Silicate (Phyll; Clay Montmorillonite Bentonite), (6) Silicate (Phyll; Clay Illite Smectite), (7) Silicate (Phyll; Serpentine Chrysotile Clinochrysot), (8) Silicate (Phyll; Serpentine Lizardite), (9) Silicate (Phyll; Clay Illite, (11) Silicate (Phyll; Clay Kaolinite), (12) Silicate (Phyll; Nontronite), (13) Sulfate; Gypsum, (14) Sulfate; Jarosite, (15) Sulfate; Kieserite, (16) Epsomite USGS GDS149, (17) Oxide; Goethite, (18) Oxide; Hematite, (19) Oxide; Magnetite, (20) Ferrihydrite USGS GDS75 Sy F6, (21) Maghemite USGS GDS81 Sy (M-3), (22) Carbonate; Calcite, (23) Carbonate; Dolomite, (24) Carbonate; Siderite, (25) Silicate (Phyll; Chlorite), (26) muscovi6.spc Muscovite GDS116 Tanzania, (27) alunite2.spc Alunite GDS83 Na63

List of atmospheric compounds:
(28) Atmosphere transmission

List of synthetic ices spectra, provided by a radiative transfert model [7]:
(29) CO2 grain size 10 000 microns, (30) H2O grain 100 microns,

List of artifact spectra:
(31) Flat 0.0001, Flat 1, (32) Slope Decreasing

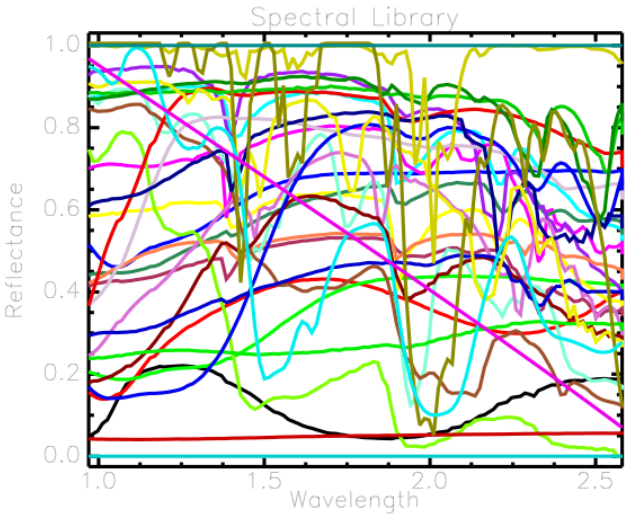

Fig 1. Spectral library containing 32 spectra (description in section 1).

2. OBSERVATION

We use the OMEGA hyperspectral detector because of its high signal-to-noise ratio [8]. We select the observation ORB0422_4 of Syrtis Major as a test case because this single cube contains well identified areas with very strong signatures of mafic minerals [10] (orthopyroxene, clinopyroxene, olivine) and phyllosilicates [11, 12]. We use 109 wavelengths within the 128 original wavelengths of the C channel (from 0.98 to 2.6 µm) and the full 128x366 pixels coverage. The cube has been radiometrically corrected using the standard correction pipeline (SOFT06) and the atmospheric gas transmission has been empirically corrected using a the volcano scan method [13,14]. We also estimate the noise variance for each observation using dark current measurements.

3. METHODS

3.1. Band Ratio

The band ratio methods and bands depth estimation are common to detect minerals on OMEGA data [9]. Unfortunately, this method is valid only if at least two wavelength channels can be identified as affected by only one particular mineral. We used here four band ratios:

$$\text{Index(Olivine)}=b2.39/b1.06 \quad (5)$$

$$\text{Index(opx)}=1-b1.84/((1.84-1.25)*b1.25+(2.47-1.84)*b2.47)*(2.47-1.25) \quad (6)$$

$$\text{Index(opx)}=1-b1.85/((2.32-1.85)*b2.32+(2.56-2.32)*b2.56)*(2.56-1.85) \quad (7)$$

$$\text{Index(phylosilicate)}=1-b1.83/((1.94-1.83)*b1.94+(2.05-1.94)*b2.05)*(2.05-1.83) \quad (8)$$

The wavelength band “b1.84” stands for the band at 1.84 microns. Orthopyroxenes are noted “opx” and clinopyroxenes are noted “cpx”.

3.2. ILSUM

The Iterative Linear Spectral Unmixing Model (ILSUM) is based on a Least squares inversion of equation 1 performed iteratively [15]. The endmember with the most negative coefficient found during the first inversion process is eliminated from the input library and the inversion is performed again with the new cleaned library. This process is repeated until no negative coefficient is found.

3.3. FCLS

This method solves the unmixing problem under non-negativity and sum-to-one constraints [16]. Since no closed form expression of the optimal abundance vector can be

derived under these two constraints, an iterative scheme is developed. The non-negativity constraint is classically handled by introducing the Lagrange function associated with the criterion to be optimized. The sum-to-one constraint is considered as an additional measurement equation leading to a new cost function. This method was previously tested to detect ices and liquid water on Mars [17]

3.4. FC-SGM

The Fully Constraint-Scale Gradient Method (FC-SGM) has been proposed in [18] as an alternative of FCLS to solve the linear unmixing problem under the non-negativity and sum-to-one constrains using the scaled gradient method The criterion to be optimized is derived from the Lagrangian formulation including the non-negativity constraint. Then this criterion is minimized thanks to an iterative scaled gradient method. The sum-to-one constraint is conveniently ensured by projecting the abundance vector onto the appropriate subspace at each iteration of the algorithm.

3.5. BPDN

We consider the Basis Pursuit De Noising (BPDN) approach [3] that solves the unmixing problem under the sparse constraint on matrix A. Sparsity is achieved by minimizing the least-squares term corresponding to (1), penalized by the L1 norm of the coefficients. A regularization parameter has to be tuned, which controls the trade-off between both terms. It is somehow related to the degree of sparsity of the solution. In the following, it was fixed to 1.
Optimization can be written as a quadratic programming problem, where positivity and sum-to-one constraints can also be taken into account. We use here the active-set strategy implemented by Matlab's medium-scale quadprog algorithm.

4. RESULTS

In table 1, we present the results of the main minerals present in the scene in comparison with the band ratio. ILSUM, FCLS and BPDN significantly detected the four minerals. Figure 2 illustrates the good match between the reference band ratio of orthopyroxene and the abundances estimated by ILSUM, FCLS and BPDN. The results from FCLS and BPDN are less noisy than ILSUM.
Table 2 indicates the computation time, of the order of several minutes for FCLS and ILSUM but significantly higher for BPDN. Table 3 presents the errors, inconsistencies and sparsity of the results. FCLS, ILSUM and BPDN have a better convergence performance, are sparser and with less negative results compared to other methods.

	Olivine	Opx	Cpx	Phyllosilicate
ILSUM	**0.84**	**0.56**	**0.77**	**0.17**
FCLS	**0.87**	**0.68**	**0.80**	**0.28**
FC-SGM	0.05	0.01	0.12	-0.01
BPDN	**0.89**	**0.53**	**0.66**	**0.26**

Table 1: Comparison of the linear unmixing results with band ratios. The proximity between both is estimated by the correlation coefficient for all pixels.

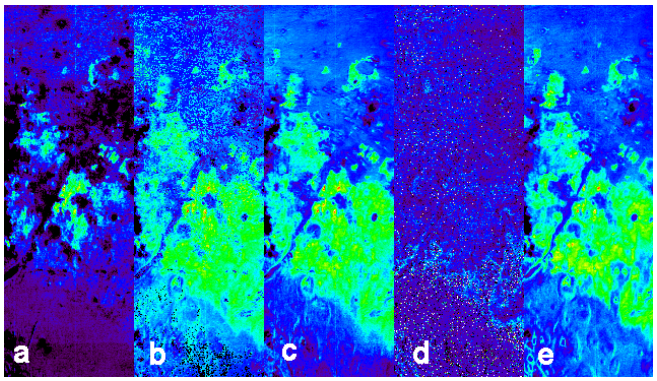

Fig 2. Image of the detection of orthopyroxene (opx). (a) reference band ratio, (b) abundance estimated with ILSUM, (c) with FCLS, (d) with FC-SGM, (e) with BPDN.

	ILSUM	FCLS	ISRA	BPDN
Time (s)	120	255	7 000	16000

Table 2: Typical computation time in seconds on a Matlab 2.53 GHz, Intel Core 2 Duo, 4Go RAM

	Conv.	< -0.01 %	> 1%	> 10%
ILSUM	**0**	**5**	18	**5**
FCLS	**0**	**5**	20	**6**
FC-SGM	**0**	32	32	32
BPDN	**0**	0	21	**8**

Table 3: Errors, inconsistency and sparsity of the results. The first column indicates the number of pixels without convergence. The other columns indicate the number of component with abundances <-0.01%, resp., >1%, resp., > 10%

5. DISCUSSION AND CONCLUSION

In our problem with a collection of 33 reference spectra and 109 wavelengths, the sparsity constraint from the BPDN method seems to be useless since the results are similar for ILSUM (without sparsity), FCLS (without sparsity) and BPDN (with sparsity). In future studies, much larger reference catalogues must be considered but, from a prior

study, neither ILSUM nor FCLS seems to be not well suited to this situation. The behavior of FC-SGM and BPDN would be studied in this situation.
Thanks to these results and the fast computation time of ILSUM and FCLS linear unmixing methods, they can be applied on large scale datasets (such as the complete OMEGA archive) in order to detect automatically the minerals at the surface on Mars [13]. The application of FC-SGM and BPDN would require a optimized implementation. We would also test recent other implementations of this problem [19].

6. ACKNOWLEDGEMENT

We would like to thank the OMEGA Team for the data management. We are grateful to USGS and the CRISM Team for providing their minerals spectral library. We are also grateful to S. Douté and B. Schmitt for their ice spectral library. This work was supported by the Centre National d'Etudes Spatiales (CNES). It is based on observations with OMEGA embarked on Mars Express. We also acknowledge partial support from the Programme National de Planétologie (CNRS/INSU).

11. REFERENCES

[1] D., Tanre et al., "Atmospheric modeling for space measurements of ground reflectances, including bidirectional properties," *Applied Optics*, vol. 18, pp. 3587– 3594, Nov. 1979.

[2] Schmidt, F., et al., , "Implementation strategies for hyperspectral unmixing using Bayesian source separation", *IEEE Transaction on Geoscience and Remote Sensing, , 48*, 4003-4013, 2010

[3] Chen, S. S., Donoho, D. L. & Saunders, M. A., "Atomic Decomposition by Basis Pursuit", *SIAM Journal on Scientific Computing, , 20*, 33-61, 1998

[4] Clark, R. N., Swayze, G. A., Wise, R., Livo, K. E., Hoefen, T. M., Kokaly, R. F. & Sutley, S. J., "USGS Digital Spectral Library splib05a", *U.S. Geological Survey, 2003*

[5] L. Le Deit, et al., "Ferric oxides in East Candor Chasma, Valles Marineris (Mars) inferred from analysis of OMEGA/Mars Express data: identification and geological interpretation", *J. Geophys. Res*, Vol. 113, No. E7, E07001, doi:10.1029/2007JE002950, 2008

[6] J.-Ph. Combe, et al., ".Analysis of OMEGA / Mars Express data hyperspectral data using a Multiple-Endmember Linear Spectral Unmixing Model (MELSUM): Methodology and first results", *Planet. Space Science,* 56, Issue 7, p. 951-975, doi:10.1016/j.pss.2007.12.007 2008

[7] S. Douté and B. Schmitt, "A multilayer bidirectional reflectance model for the analysis of planetary surface hyperspectral images at visible and near-infrared wavelengths," *J. Geophysical Research*, vol. 103, no. 12, pp. , 1998

[8] J.-P. Bibring et al., "OMEGA: Observatoire pour la Minéralogie, l'Eau, les Glaces et l'Activité". *ESA SP- 1240*, Aug. 2004, ch. Mars Express: the Scientific Payload, pp. 37–49.

[9] Bibring, J.-P., et al., "Mars Surface Diversity as Revealed by the OMEGA/Mars Express Observations", *Science, 307*, 1576-1581, 2005

[10]Mustard, J. F.; Poulet, F.; Gendrin, A.; Bibring, J.-P.; Langevin, Y.; Gondet, B.; Mangold, N.; Bellucci, G.; Altieri, F. "Olivine and Pyroxene Diversity in the Crust of Mars", *Science*, Volume 307, Issue 5715, pp. 1594-1597 (2005)

[11] Poulet, F.; Bibring, J.-P.; Mustard, J. F.; Gendrin, A.; Mangold, N.; Langevin, Y.; Arvidson, R. E.; Gondet, B.; Gomez, C. , "Phyllosilicates on Mars and implications for early martian climate", *Nature*, Volume 438, Issue 7068, pp. 623-627 (2005).

[12] Ehlmann, B. L., et al, "Identification of hydrated silicate minerals on Mars using MRO-CRISM: Geologic context near Nili Fossae and implications for aqueous alteration", *J. Geophys. Res., AGU, 114*, E00D08-, 2009

[13] Erard, S., Calvin, W., "New composite spectra of Mars", 0.4–5.7 mm. *Icarus* 130, 449–460, 1997

[14] Langevin, Y., Poulet, F., Bibring, J.P., gondet, B., "Sulfates in the North Polar Region of Mars Detected by OMEGA/Mars Express", *Science*, vol 307, p1584-1586, 2005

[15] S. Le Mouélic, et al., "An iterative least squares approach to decorrelate minerals and ices contributions in hyperspectral images : application to Cuprite (Earth) and Mars", *2009. WHISPERS,* 26-28 Aug. 2009, DOI10.1109/WHISPERS.2009.5289003

[16] D. Heinz and C.-I. Chang, "Fully constrained least squares linear mixture analysis for material quantification in hyperspectral imagery," *IEEE Transactions on Geoscience and Remote Sensing*, vol. 39, pp. 529–545, 2000.

[17] Kereszturi, A., Vincendon, M. & Schmidt, F., "Water ice in the dark dune spots of Richardson crater on Mars ", *Planetary and Space Science, , 59*, 26-42, 2011

[18] Theys, C., Dobigeon, N., Tourneret, J.-Y. & Lantéri, H., "Linear unmixing of hyperspectral images using a scaled gradient method", *Proc. IEEE Workshop on Statistical Signal Processing (SSP),* 729-732, 2009

[19] M.-D. Iordache, J. Bioucas-Dias and A. Plaza, "Sparse unmixing of hyperspectral data", *IEEE Transactions on Geoscience and Remote Sensing*, 2011 (in press).